EPJ Web of Conferences **146**, 11027 (2017) DOI: 10.1051/epjconf/201714611027
ND2016

Neutron production in deuteron-induced reactions on Li, Be, and C at an incident energy of 102 MeV

Shouhei Araki[1], Yukinobu Watanabe[1,a], Mizuki Kitajima[1], Hiroki Sadamatsu[1], Keita Nakano[1], Tadahiro Kin[1], Yosuke Iwamoto[2], Daiki Satoh[2], Masayuki Hagiwara[3], Hiroshi Yashima[4], and Tatsushi Shima[5]

[1] Department of Advanced Energy Engineering Science, Kyushu University, 6-1 Kasuga-koen, Kasuga, Fukuoka 816-8580, Japan
[2] Japan Atomic Energy Agency (JAEA), 2-4 Shirakata, Tokai, Naka, Ibaraki 319-1195, Japan
[3] High Energy Accelerator Research Organization (KEK), 1-1 Oho, Tsukuba, Ibaraki 305-0801, Japan
[4] Research Reactor Institute, Kyoto University, 2-1010 Asashiro-nishi, Kumatori, Sennan, Osaka 590-0494, Japan
[5] Research Center for Nuclear Physics (RCNP), Osaka University, 10-1 Mihogaoka, Ibaraki, Osaka 567-0047, Japan

Abstract. Double-differential cross sections (DDXs) of deuteron-induced neutron production reactions on Li, Be, and C at 102 MeV were measured at forward angles ($\leq 25^{\circ}$) by means of a time of flight method with NE213 liquid organic scintillators at the Research Center of Nuclear Physics, Osaka University. The experimental results were compared with model calculations with PHITS and DEURACS. The DEURACS calculation reproduces the experimental DDXs for C at very forward angles than the PHITS one. Moreover, the incident energy dependence of the Li(d,xn) reaction was investigated by adding the DDX data measured previously at 25 and 40 MeV.

1. Introduction

The (d,xn) reaction on Li, Be, and C is considered as one of the effective reactions to produce high intensity neutron beams necessary in modern neutron applications such as radiation damage evaluation for fusion materials [1], medical radioisotope production [2], and nuclear transmutation studies [3]. Some neutron beam facilities are under construction or design, e.g., the international Fusion Material Irradiation Facility (IFMIF) [1], the neutron for Science (NFS) facility at SPIRAL2 [4] and the Beijing Isotope Separation On-Line neutron beam facility (BISOL) [5]. In the engineering design of such neutron source facilities, it is important to make reliable assessment of neutron yields from Li, Be, and C used as neutron converter. Therefore, basic nuclear data that can describe accurately deuteron-induced neutron production reactions are required for the assessment of neutron yields.

Some theoretical model codes for deuteron-induced reactions are currently available. For example, the Liege Intra-Nuclear Cascade model (INCL) [6] has been implemented in PHITS [7]. Also, DEUteron-induced Reaction Analysis Code System (DEURACS) is being developed [8,9]. The latest work has demonstrated that DEURACS calculations reproduce well experimental thick target neutron yields (TTNYs) data of (d,xn) reactions on Be and C for incident energies below 50 MeV. However, validation of INCL and DEURACS has not been sufficient for deuteron-induced neutron production over a wide range of incident energy.

Under these situations, experimental deuteron-induced neutron production data are required to validate nuclear reaction models. Double-differential neutron production cross sections (DDXs) are especially indispensable not only for characterization of neutron sources, but also for understanding the reaction mechanism and in the development of reliable theoretical models. However, available experimental DDX data are very limited and no data exist above 50 MeV.

In the present work, we have performed a new measurement of DDXs for deuteron-induced neutron production reactions on three target nuclei, Li, Be, and C, at 102 MeV. The measured data are compared with PHITS and DEURACS calculations. Moreover, the incident energy dependence of the Li(d,xn) reaction is investigated using the previous measurements at 25 and 40 MeV [10,11], in comparison with the Li(p,n) data in the incident energy range from 20 to 140 MeV.

2. Experimental method

The experiment with a time of flight (TOF) method was performed at the ring cyclotron facility of the Research Center for Nuclear Physics (RCNP), Osaka University. It was carried out at the same time that the measurement of (d,xn) reactions on Al, Cu, and Nb [12]. The experimental setup was almost the same as used in the (p,xn) measurements at the RCNP [13,14].

The experimental arrangement is shown in Fig. 1. A deuteron beam was accelerated up to 102 MeV by the ring cyclotron, and pulsed at 1.09 MHz using a beam chopper. The deuteron beam bombarded a thin target placed in the beam swinger magnet and then delivered to a Faraday cup. The beam current was changed from 5 to 20 nA, depending on target and measurement angle. The following targets were used: Li (its thickness: 53 mg/cm^2), Be (33.9 mg/cm^2), and C (14.0 mg/cm^2). Energy spectra of neutrons emitted from the targets were measured

[a] e-mail: watanabe@aees.kyushu-u.ac.jp

 DOI: 10.1051/epjconf/201714611027

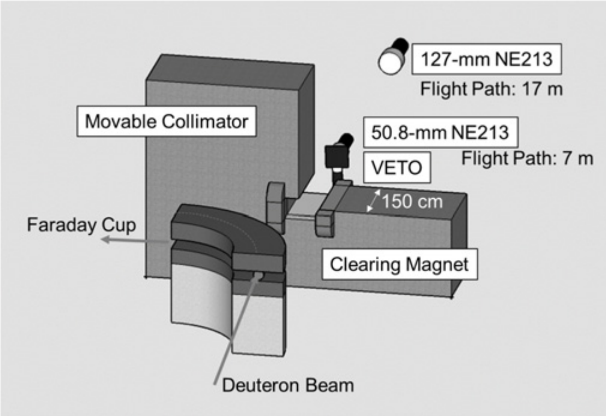

Figure 1. Experimental setup.

at angles of 0°, 5°, 10°, 15°, 20°, and 25° for Be and C, and 0° and 10° for Li, by moving the target along the beam trajectory in the swinger magnet. The emitted neutrons were transported to the 100-m TOF tunnel through a movable collimator. The position of the collimator was changed depending on the target position. A clearing magnet was installed in the collimator to remove background components of charged particles.

The energies of emitted neutrons were measured by the TOF method with two different sizes of NE213 liquid organic scintillators (50.8 mm by 50.8 mm and 127 mm by 127 mm in diameter and length). The 50.8-mm and 127-mm detectors were placed at 7 m and 17 m from the target, respectively. Since the magnetic field of the clearing magnet influenced the photomultiplier tube at 7 m, the magnet was switched off and a 5-mm thick NE102A plastic scintillator was additionally mounted in front of the 50.8-mm NE213 detector as a veto detector of background charged particles.

3. Data analysis

The light outputs from the NE213 detectors were calibrated with gamma-rays from ^{137}Cs and ^{241}Am/Be radioactive sources, and the thresholds of the 50.8-mm and 127-mm detectors were set to be 0.49 MeVee and 4.3 MeVee, respectively.

In the low energy range ($\leq$15 MeV), the number of background gamma-ray events was comparable to that of neutron events in the measurement with the 50.8 mm NE213 detector. Both the events were well separated by the pulse shape discrimination method [15]. Neutron events were clearly distinguished from gamma-ray events in the light output range above the detector bias 0.49 MeV.

To obtain the absolute neutron flight time, the prompt gamma peak observed in the measured TOF spectrum was used as a reference point. The neutron energy was calculated from the flight time, and the TOF spectrum was converted to the energy spectrum.

The experimental DDX was derived from the energy spectrum using the target thickness, the solid angle subtended by the detector, the deuteron beam current, the neutron detection efficiency, and the attenuation correction of neutron fluxes. The neutron detection efficiencies were calculated with the SCINFUL-QMD code [16,17]. The attenuation of neutron fluxes in air at 7 m and 17 m was estimated by the PHITS code with JENDL/HE-2007 [18].

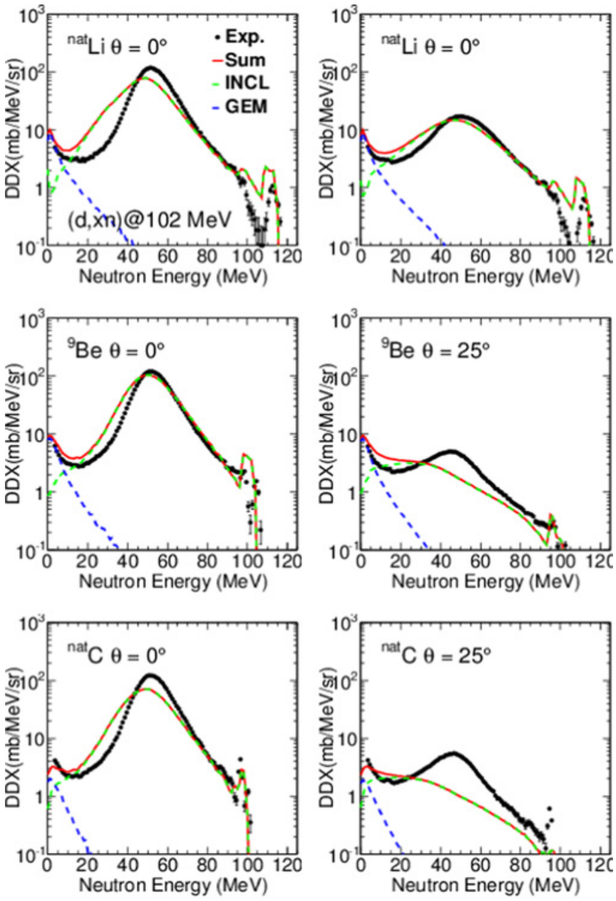

Figure 2. Comparison of measured DDXs at 0° and 10° for Li and at 0° and 25° for Be and C and PHITS calculations.

Finally, both the DDXs measured at 7 m and 17 m were merged at 15 MeV.

Uncertainties of the measurements are due to systematic and statistical errors. The systematic errors are as follow: (a) the accuracy of the detection efficiencies calculated by the SCINFUL-QMD code, (b) the uncertainty in the PSD, (c) the determination of the solid angle, (d) the integrated beam current, (e) the accuracy of the correction of attenuation in air estimated by the PHITS code, and (f) the influence of neutron scattering from the swinger magnet, the floor, the wall, and the collimator. As a result, the total systematic error was estimated to be 11 to 12%.

4. Results and discussion

4.1. Experimental results

The measured DDXs at 0° and 10° for Li and at 0° and 25° for Be and C are shown in Fig. 2. A broad peak around half of the incident energy (~50 MeV) and discrete peaks at the high-energy end (~100 MeV) are observed for each target. The broad peak is known to originate from elastic and non-elastic deuteron breakup reactions. The discrete peaks correspond to the transition to low-lying discrete levels in the residual nucleus by single-proton transfer reactions.

4.2. Comparison with PHITS calculations

The PHITS code has some model options for the total reaction cross section, the dynamical and the

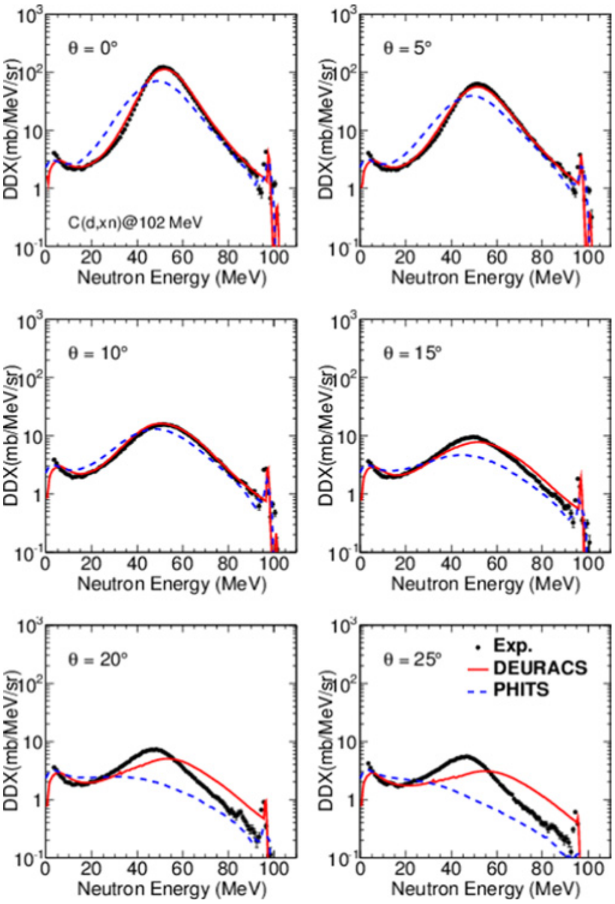

Figure 3. Comparison of measured DDXs for C at emission angles from 0° to 25° with DEURACS and PHITS calculations.

subsequent evaporation processes. In the present work, the KUROTAMA model [19] was chosen for calculation of the total reaction cross section. INCL4.6 and the generalized evaporation model (GEM) [20] were employed in simulating the dynamical process including deuteron breakup reaction and the subsequent evaporation process, respectively.

The PHITS calculations are shown by the lines in Fig. 2. In the low energy region, the GEM component is dominant, showing close agreement with the experimental data. The INCL component gives the broad peak seen around 50 MeV at very forward angles although the calculated peak shape is broader than the experimental one. On the other hand, the PHITS calculations cannot reproduce the observed broad peak at 25°. The discrete peak at the high-energy end is not correctly reproduced by the INCL.

4.3. Comparison with DEURACS calculations

In DEURACS, elastic and non-elastic breakup reactions are described by the continuum discretized coupled channel theory and the Glauber model, respectively. In addition, the Distorted Wave Born Approximation (DWBA) is employed for single-proton transfer reactions to bound states in the residual nuclei.

The DDXs for C at 0° to 25°Calculated by DEURACS are shown in Fig. 3. The PHITS calculations are also plotted for comparison. The DEURACS calculations are in excellent agreement with the experimental data at very forward angles from 0° to 15°, and reproduce the broad peak perfectly. However, the calculated peak positon at 20° and 25° is shifted to higher emission energy compared to the experimental data.

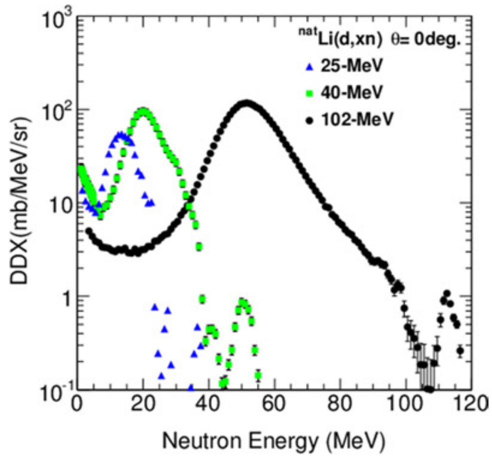

Figure 4. Measured double differential cross sections for the Li(d,xn) reactions at 25 MeV [10], 40 MeV [11], and 102 MeV.

Table 1. Parameters of the broad peak.

Ed [MeV]	Peak height [mb/sr/ MeV]	Peak energy [MeV]	FWHM [MeV]	FWHM/ peak energy [%]
25	54.6	13.2	9.00	68.1
40	95.8	20.0	10.4	52.0
102	117	51.6	17.4	33.7

4.4. Energy dependence of the Li(d,xn) reaction

4.4.1. Double-differential cross sections at 0°

The measured DDXs for Li at 102 MeV are compared with the measured ones at 25 MeV [10] and 40 MeV [11] in Fig. 4. The characteristic broad peak around half of the incident energy is also observed at low incident energies of 25 MeV and 40 MeV.

To investigate the incident energy dependence of the measured DDXs at 0°, the observed broad peak was characterized by the peak height, the peak energy, the FWHM, and the ratio of the FWHM to the peak energy. Those parameters are summarized in Table 1. Three of them (the peak height, the peak energy, and the FWHM) increase with incident energy, while the ratio of FWHM to peak energy decreases. This decreasing trend indicates that the spectral shape is sharper with incident energy. Therefore, the mono-energetic property of neutron production in the Li(d,xn) reaction is expected to be gradually better as the incident energy increases.

4.4.2. Differential cross section at 0°

Figure 5 shows the experimental differential cross sections (DXs) at 0° for the Li(d,xn) and Li(p,n) reactions. The DXs of the Li(d,xn) reaction were derived by integrating the DDXs within the FWHM around the observed broad peak. The DXs of the ^{7}Li(p,n)^{7}Be reaction measured in Refs. [14,22,23] include both transitions to the ground and the first excited states of the residual nucleus. It is found that neutron production in the Li(d,xn) reaction

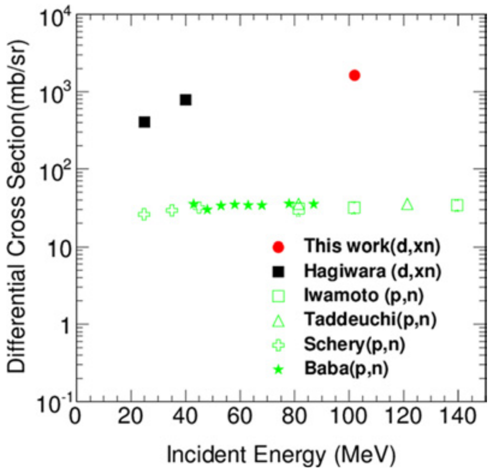

Figure 5. Measured differential cross section at 0° for the Li(d,xn) reactions and ^{7}Li(p,$n_{0,1}$)^{7}Be reactions at incident energies between 25 to 140 MeV.

is larger than that in the ^{7}Li(p,n)^{7}Be reaction by more than an order of magnitude. As for the incident energy dependence, the DXs of the Li(d,xn) reaction increase gradually with increasing incident energy, while the DXs of the ^{7}Li(p,n)^{7}Be reaction has almost constant value (∼36 mb/sr) at incident proton energies between 20 to 140 MeV.

5. Summary and conclusions

The double-differential cross sections (DDXs) of 102 MeV (d,xn) reactions on Li, Be, and C were measured at forward angles from 0° to 25° by the TOF method. The measured DDXs were compared with the PHITS and DEURACS calculations. The PHITS calculations reproduced generally the measured DDXs at very forward angles. However, the calculated broad peak around 50 MeV was found to be wider than the measured one. On the other hand, the DEURACS calculations showed excellent agreement with the measured DDXs for C over a wide range of emission energies at small angles from 0° to 15°.

The energy dependence of neutron production at 0° was investigated from comparison of the Li(d,xn) and Li(p,n) reactions. It was found that the broad peak around half of the incident energy observed in the Li(d,xn) reaction becomes relatively sharper and the differential cross sections at 0° show a gradual increase as the incident energy increase.

The authors wish to thank the staff of the RCNP for providing high-quality deuteron beams and for their assistance during the experiment. They are grateful to thank S. Nakayama for his DEURACS calculations. They also thank S. Hashimoto for useful discussion on INCL calculation in PHITS. This work was partly funded by the Sasakawa Scientific Research Grant from The Japan Scientific Society (28–210). S.A. is grateful to the Kyushu industrial technology center for financial support for participation in this conference.

References

[1] A. Moeslang, V. Heinzel H. Matsui, M. Sugimoto, Fusion Eng. Des. **81**, 863 (2006)
[2] Y. Nagai, K. Hashimoto, Y. Hatsukawa et al., Jour. Phys. Soc. Japan **82**, 064201 (2013)
[3] Implication of Partitioning and Transmutation in Radioactive Waste Management, IAEA Technical Reports Series No. 435 (2004)
[4] M. Fadil, B. Rannou, Nucl. Instrum. Meth. B **226**, 4318 (2008)
[5] S.X. Peng, F. Zhu, Z. Wang et al., Nucl. Instrum. Meth. B **376**, 420 (2016)
[6] A. Boudard, J. Cugnon, J.C. David, et al. Phys. Rev. C **87**, 014606 (2013)
[7] T. Sato, K. Niita, N. Matsuda, et al. J. Nucl. Sci. Tech. **50**, 913 (2013)
[8] S. Nakayama, Y. Watanabe, J. Nucl. Sci. Tech. **53**, 913 (2016)
[9] S. Nakayama, H. Kouno, Y. Watanabe et al., Phys. Rev. C **94**, 014618 (2016)
[10] M. Hagiwara, T. Itoga, T. Oishi, et al., Jour. Nucl. Mater **417**, 1284 (2011)
[11] M. Hagiwara, T. Itoga, N. Kawata, et al. Fus. Sci. Tech. **48**, 1320 (2005)
[12] S. Araki, Y. Watanabe, M. Kitajima, et al., Nucl. Instrum. Meth. A **842**, 62 (2017)
[13] Y. Iwamoto, S. Taniguchi, N. Nakao, et al., Nucl. Instrum. Meth. A **598**, 298 (2008)
[14] Y. Iwamoto, M. Hagiwara, D. Satoh, et al., Nucl. Instrum. Meth. A **804**, 50 (2015)
[15] M. Moszynski, G.J. Costa, G. Guillaume, et al., Nucl. Instrum. Meth. A **343**, 563 (1994)
[16] D. Satoh, T. Sato, N. Shigyo, et al., JAEA-Data/Code **2006-023** (2006)
[17] D. Satoh, T. Sato, A. Endo, et al., J. Nucl. Sci. Tech. **43**, 714 (2006)
[18] Y. Watanabe, T. Fukahori, K. Kosako, et al., AIP Conf. Proc. **769**, 326 (2005)
[19] K. Iida, A. Kohama, K. Oyamatsu, Jour. Phys Soc. Japan **76**, 044201 (2007)
[20] S. Furihata, Nucl. Instrum. Meth. B **171**, 251 (2000)
[21] T.N. Taddeuchi, C.A. Goulding T.A. Carey, et al., Nucl. Phys. A **469**, 125 (1987)
[22] S. Schery, L. Young, R. Doering, et al., Nucl. Instrum. Meth. **147**, 399 (1977)
[23] M. Baba, Y. Nauchi, T. Iwasaki, et al., Nucl. Instrum. Meth. A **428**, 454 (2000)